BIODIVERSITAS
Volume 27, Number 5, May 2026
Pages: 14

ISSN: 1412-033X
E-ISSN: 2085-4722
https://doi.org/10.13057/biodiv/d270516

Phytochemical profile, antioxidant potential, and antibacterial activity of Thai polyherbal formulation, a Ya Kae Rok Bit remedy

CHAWALIT YONGRAM[1], PALAPON CHIMPALEE[2], SUWADEE CHOKCHAISIRI[2], SASIPEN KRUTCHANGTHONG[3], JIRAPORN SONGSRI[4], THAVATCHAI KAMOLTHAM[2], PANUPAN SRIPAN[2,♥]

[1]National Institute of Nuclear and Radiation Reference Standards Laboratory, Office of Atoms for Peace. 16 Vibhavadi Rangsit Road, Chatuchak 10900, Bangkok, Thailand

[2]Division of Cannabis Health Sciences, College of Allied Health Sciences, Suan Sunandha Rajabhat University. 111/1-3 Rama 2 Road, Mueang Samut Songkhram 75000, Samut Songkhram, Thailand. Tel.: +66-34-773-905, ♥email: panupan.sr@ssru.ac.th

[3]Division of Applied Thai Traditional Medicine, College of Allied Health Sciences, Suan Sunandha Rajabhat University. 111/1-3 Rama 2 Road, Mueang Samut Songkhram 75000, Samut Songkhram, Thailand

[4]Division of Applied Thai Traditional Medicine, Faculty of Science and Technology, Phranakorn Rajabhat University. 9 Chaengwattana Rd., Bang Khen 10220, Bangkok, Thailand

Manuscript received: 5 March 2026. Revision accepted: 11 May 2026.

Abstract. *Yongram C, Chimpalee P, Chokchaisiri S, Krutchangthong S, Songsri J, Kamoltham T, Sripan P. 2026. Phytochemical profile, antioxidant potential, and antibacterial activity of Thai polyherbal formulation, a Ya Kae Rok Bit remedy. Biodiversitas 27 (5): d270516. https://doi.org/10.13057/biodiv/d270516*. This study investigated the quantitative and qualitative phytochemical diversity and biological activities of Ya Kae Rok Bit (YKRB) extracts prepared using different solvents (hexane, ethyl acetate, and ethanol). Total phenolic, flavonoid, and tannin contents were also evaluated. Antioxidant capacity was evaluated using DPPH, ABTS, and FRAP assays, while antibacterial activity against *Escherichia coli* ATCC 25922 and *Staphylococcus aureus* ATCC 25923 was determined by disc diffusion and broth microdilution. GC-MS analysis identified 28 phytochemical constituents, including neutral cannabinoids, with tetrahydrocannabinol (23.24-27.91%) and cannabinol (14.18-21.06%) as relatively abundant compounds based on peak area normalization, together with macelignan (6.34-10.55%). HPLC confirmed the highest Δ9-THC content in the hexane extract (6.92 mg/g extract). The extracts showed measurable antioxidant activity in the DPPH assay (IC_{50} = 56.72-95.25 µg/mL) and stronger radical scavenging activity in the ABTS assay (IC_{50} = 23.26-26.93 µg/mL), with reducing capacity observed in the FRAP assay (200.92 mmol Fe^{2+}/100 g extract). Moreover, YKRB showed antibacterial activity against *S. aureus* (MIC = 25 mg/mL), while no activity was observed against *E. coli*. These findings demonstrate solvent-dependent phytochemical variation and provide preliminary evidence of antioxidant and selective antibacterial activities of YKRB extracts.

Keywords: Antioxidant activity, cannabinoids, *Cannabis sativa*, polyherbal remedy, traditional herbal medicine

INTRODUCTION

Diarrheal diseases remain a major public health concern worldwide, particularly in low- and middle-income countries where enteric infections are still prevalent. Although microbial pathogens represent the primary cause, oxidative stress has also been implicated in intestinal dysfunction. Oxidative stress has been associated with disruption of epithelial barrier integrity and activation of inflammatory signaling pathways, contributing to gastrointestinal dysfunction (WHO 2023; Jin et al. 2024; Rezvani et al. 2024). These conditions continue to encourage the exploration of complementary therapeutic approaches, including medicinal plants and traditional polyherbal formulations that contain chemically diverse bioactive compounds.

Traditional medical systems frequently employ complex plant-based remedies developed through long-standing empirical practice. In Thai Traditional Medicine (TTM), diarrhea is interpreted as a disorder associated with an imbalance of the Uccāra-dhātu, which governs intestinal excretion and digestive equilibrium (Thai Traditional Medicine Institute 2025). Investigation of traditional formulations may therefore provide useful ethnopharmacological information for modern phytochemical and biological studies.

Ya Kae Rok Bit (YKRB) is a classical Thai polyherbal remedy traditionally used for more than two centuries to relieve diarrhea and gastrointestinal discomfort. The formulation comprises fourteen plant-derived ingredients, with *Cannabis sativa* L. together with medicinal spices such as *Allium sativum* L., *Zingiber officinale* Roscoe, and *Piper nigrum* L. (Department of Thai Traditional and Alternative Medicine 2021). These plants contain diverse secondary metabolites such as cannabinoids, terpenoids, phenolics, alkaloids, and fatty acid derivatives, which may contribute to multiple biological activities.

Previous studies have reported that cannabinoids such as Δ9-tetrahydrocannabinol (Δ9-THC), cannabidiol (CBD), and cannabinol (CBN) exhibit antibacterial activity, particularly against Gram-positive bacteria, and may modulate inflammatory pathways through cannabinoid receptor signaling (Farha et al. 2020; Crowley et al. 2024). Phytochemicals from other ingredients of the formulation, including *A. sativum*, *Z. officinale*, and *P. nigrum*, also

possess documented antioxidant and antimicrobial activities (Bhatwalkar et al. 2021; Alves et al. 2023). However, most previous investigations have focused on individual medicinal plants, whereas systematic phytochemical characterization and biological evaluation of the complete YKRB polyherbal formulation remain limited.

This study aimed to systematically characterize the YKRB formulation using integrated phytochemical and biological approaches. Extracts obtained using solvents with different polarities were evaluated to investigate solvent-dependent chemical diversity and associated biological activities. Antioxidant activity was determined using DPPH, ABTS, and FRAP assays, whereas antibacterial activity was evaluated against *Escherichia coli* ATCC 25922 and *Staphylococcus aureus* ATCC 25923. Chemical profiling was conducted using GC-MS and HPLC, and in silico pharmacokinetic prediction was performed to assess the drug-likeness of selected compounds. This study provides an integrated evaluation of YKRB through multi-solvent extraction, phytochemical profiling, biological screening, and computational ADME prediction, while not directly assessing antidiarrheal pharmacological effects.

MATERIALS AND METHODS

Preparation of YKRB remedy and mineral detoxification

Plant materials (No.2-14) of the YKRB formulation (Table 1) were obtained from Thaprachan Herbal Shop (Healthy Hills Farm Company Limited), Phasi Charoen District, Bangkok 10160, Thailand (13.72361°N, 100.46050°E), a certified supplier of traditional Thai herbal materials. All plant materials were authenticated based on macroscopic and organoleptic characteristics in accordance with the Thai Herbal Pharmacopoeia (Ministry of Public Health 2016) before formulation preparation. For *C. sativa*, (No. 1 in Table 1) used as a component of the YKRB formulation, was cultivated under controlled conditions in a licensed indoor cultivation facility located in Bang Kaeo Sub-district, Mueang Samut Songkhram District, Samut Songkhram Province, Thailand (13.41993°N, 100.03920°E). The *cannabis* material was produced under a narcotics category-5 cultivation and production license (No. 22/2563) approved by the Thai Food and Drug Administration (FDA), Ministry of Public Health, Royal Thai Government. Plant materials were collected in May 2022 from the facility. The use of *C. sativa* in this study complied with the Narcotics Act B.E. 2522 (1979) and its Amendment (No. 7) B.E. 2562 (2019) (Royal Thai Government Gazette 2019), and the research activities were conducted under the regulatory oversight of the Thai Food and Drug Administration and the Ministry of Public Health, Thailand. Scientific names were verified using Plants of the World Online (POWO 2024). Voucher specimens were deposited at the Division of Cannabis Health Sciences, Suan Sunandha Rajabhat University, Samut Songkhram, Thailand. The formulation comprised fourteen components (Table 1).

Three mineral ingredients in the YKRB formulation were detoxified using the traditional Thai *satu* method before formulation preparation. Each mineral was processed separately by heating approximately 50 g in a heat-resistant earthenware vessel over a controlled charcoal furnace at approximately 200-300°C for 45-60 min. Heating was continued until the material reached a semi-liquid or molten texture. The endpoint of the *satu* process was determined by visual observation of softening and partial liquefaction. After cooling to room temperature, the processed minerals were ground into fine powder before incorporation into the YKRB formulation. The YKRB formulation was prepared with a mixture of plant materials and mineral ingredients, following the proportions in Table 1, and kept at 25°C before extraction.

Table 1. Composition of YKRB remedy

No.	Scientific name (Family)	Part used	Proportion (%)	Collector No.	Voucher No.
1	*Cannabis sativa* L. (Cannabaceae)	Inflorescence	50	P. Sripan 009	PS.47
2	*Allium sativum* L. (Amaryllidaceae)	Bulb	3.33	P. Sripan 023	PS.75
3	*Curcuma zedoaria* (Christm.) Roscoe (Zingiberaceae)	Rhizome	3.33	P. Sripan 020	PS.72
4	*Zingiber officinale* Roscoe (Zingiberaceae)	Rhizome	3.33	P. Sripan 003	PS.41
5	*Zingiber purpureum* Roscoe (Zingiberaceae)	Rhizome	3.33	P. Sripan 017	PS.55
6	*Piper nigrum* L. (Piperaceae)	Fruit	3.33	P. Sripan 010	PS.48
7	*Terminalia triptera* Stapf (Combretaceae)	Fruit	3.33	P. Sripan 021	PS.73
8	*Clerodendrum indicum* (L.) Kuntze (Lamiaceae)	Leaf	3.33	P. Sripan 022	PS.74
9	*Allium cepa* L. (Amaryllidaceae)	Bulb	3.33	P. Sripan 019	PS.71
10	*Myristica fragrans* Houtt. (Myristicaceae)	Nut	6.67	P. Sripan 015	PS.53
11	*Myristica fragrans* Houtt. (Myristicaceae)	Mace	6.67	P. Sripan 012	PS.50
12	Sulfur (processed by *satu*)*	Mineral material	3.33	-	-
13	Potassium nitrate (processed by *satu*)*	Mineral material	3.33	-	-
14	Potassium alum (processed by *satu*)*	Mineral material	3.33	-	-

Note: *Satu** is a traditional Thai detoxification method involving moderate heat treatment to reduce toxicity of mineral materials before incorporation into the formulation

Preparation of crude extracts

Dried plant materials used in the YKRB formulation were ground and mixed according to the prescribed formulation ratios. The blended material was homogenized as a single batch and sieved to obtain a uniform particle size before extraction.

For extraction, 50 g of the powdered mixture was extracted with hexane, ethyl acetate (EtOAc), and ethanol (EtOH) as a commercial grade using ultrasound-assisted extraction (GT SONIC-D3 ultrasonic bath, 100 W, 40 kHz; Guangdong GT Sonic Co., China) at room temperature (25-28°C). Each extraction was performed with 100 mL of solvent for 20 min per cycle with three consecutive extraction cycles. The filtrates obtained from the three extraction cycles were combined and filtered through Whatman No. 1 filter paper before solvent removal.

The filtrates were concentrated under reduced pressure using a rotary evaporator (Rotavapor® R-210, Büchi, Switzerland) at temperatures below 50°C to minimize thermal degradation of heat-sensitive phytochemicals. The extracts were dried to constant weight and stored at −10°C in light-protected containers until further analyses were performed. Extraction yield (%) was calculated using the following equation:

$$\text{Extraction yield } (\%) = \left(\frac{W_1}{W_0}\right) \times 100$$

Where, W_1 is the weight of the dried crude extract and W_0 is the initial dry weight of the powdered mixture.

Chemical composition

Determination of Total Phenolic Content (TPC)

Total phenolic content was determined using the Folin-Ciocalteu method. Briefly, the extract at 2000 µg/mL (20 µL) was mixed with 10% Folin-Ciocalteu reagent (100 µL), followed by 7% sodium carbonate solution (80 µL). After incubation at room temperature for 30 min, absorbance was measured at 760 nm using a microplate reader (SPECTROstar® Nano, BMG LABTECH, Germany). Gallic acid was used as a reference standard. Results were expressed as mg gallic acid equivalents per gram of extract (mg GAE/g extract) based on a standard curve of gallic acid (1-30 µg/mL, y = 0.0524x - 0.0137; R^2 = 0.999). The experiments were performed in triplicate (n = 3) (Asyhar et al. 2023).

Determination of Total Flavonoid Content (TFC)

Total flavonoid content was evaluated using the aluminum chloride colorimetric method. Extracts at 500 µg/mL were mixed with 2% $AlCl_3$ solution in a 1:1 (v/v) ratio and incubated for 20 min at room temperature. Absorbance was measured at 415 nm using a microplate reader. Quercetin was used as a reference standard. Results were expressed as mg quercetin equivalents per gram of extract (mg QE/g extract) based on a standard curve of quercetin (1-20 µg/mL, y = 0.0425x + 0.0542; R^2 = 0.9989). The experiments were performed in triplicate (n = 3) in the same extract (Asyhar et al. 2023).

Determination of Total Tannin Content (TTC)

Total tannin content was determined using a modified Folin-Ciocalteu colorimetric assay developed by Gomes et al. (2021). Briefly, extracts at 500 µg/mL (20 µL) were mixed with distilled water (70 µL), 10% Folin-Ciocalteu reagent (55 µL) and 7% sodium carbonate solution (55 µL), followed by incubation for 30 min at room temperature. Absorbance was measured at 760 nm using a microplate reader. Tannin content was expressed as mg tannic acid equivalents per gram of extract (mg TAE/g extract) on the basis of a standard curve of tannic acid (1-50 µg/mL, y = 0.0226x + 0.0257; R^2 = 0.9964). The experiments were performed in triplicate (n = 3) in the same extract.

GC-MS analysis

Gas Chromatography-Mass Spectrometry (GC-MS) analysis was conducted using a Shimadzu QP-2010 system (Shimadzu, Kyoto, Japan) equipped with a J&W DB-5MS capillary column (30 m × 0.25 mm i.d., 0.25 µm film thickness; Agilent Technologies, USA). Helium (99.999% purity, grade 5.5) was employed as the carrier gas at a constant flow rate of 1.0 mL/min. The oven temperature program was as follows: initial temperature 70°C (held for 2 min), ramped at 10°C/min to 200°C, then increased at 5°C/min to 320°C and held for 10 min. The injector temperature was maintained at 250°C. Samples (1 µL) were injected in split mode with a split ratio of 1:20. Mass spectrometric detection was performed under Electron Impact (EI) ionization at 70 eV. The ion source temperature was set at 200°C, the interface (transfer line) temperature at 280°C, and the quadrupole temperature at 150°C. Mass spectra were acquired in full scan mode over an m/z range of 40-600 with a solvent delay of 3 min. Compound identification was achieved by comparison of mass spectra with those in the NIST17 mass spectral library and by calculation of Retention Indices (RI) relative to a homologous series of n-alkanes analyzed under identical chromatographic conditions. Only compounds with spectral similarity indices ≥ 80% and consistent retention index agreement were considered tentatively identified (Yongram et al. 2025). Relative composition was expressed as percentage peak area normalization and should be considered semi-quantitative.

HPLC analysis

Cannabinoid analysis was performed using a C18 reversed-phase column (150 × 4.6 mm, 2.7 µm). The mobile phase consisted of 0.085% (v/v) phosphoric acid in water (A) and 0.085% (v/v) phosphoric acid in acetonitrile (B). Separation was achieved under gradient elution starting at 70% B (0-3 min), increased to 85% B (3-7 min), increased to 95% B (7-8 min), followed by re-equilibration to 70% B until 12 min. The chromatographic system operated at a flow rate of 1.6 mL/min with the column temperature maintained at 35°C. Samples were injected at a volume of 5 µL, and detection was carried out at 220 nm. Under the described chromatographic conditions, the identified cannabinoids were eluted at distinct retention times as follows: cannabidivarin (CBDV) at 2.65 min,

cannabidiolic acid (CBDA) at 3.53 min, cannabigerolic acid (CBGA) at 3.85 min, cannabigerol (CBG) at 4.05 min, cannabidiol (CBD) at 4.20 min, tetrahydrocannabivarin (THCV) at 4.32 min, cannabinol (CBN) at 5.85 min, Δ9-tetrahydrocannabinol (Δ9-THC) at 6.70 min, and cannabichromene (CBC) at 7.60 min. These well-resolved peaks confirm chromatographic separation and support analytical reproducibility under the applied conditions. The overall chromatographic conditions and validation framework were adapted from the previously reported HPLC protocol of Chokchaisiri et al. (2026).

The quantified cannabinoids included CBGA, CBG, CBDA, CBD, THCA, Δ9-THC, CBC, CBN, CBDV, and THCV, using certified reference standards for external calibration. Calibration curves showed excellent linearity ($R^2 > 0.999$). Limits of Detection (LOD) and quantification (LOQ) were determined at signal-to-noise ratios of 3:1 and 10:1, respectively (Table 2). Method validation parameters were established following the HPLC protocol reported by Chokchaisiri et al. (2026). Precision was evaluated by replicate injections, yielding relative standard deviations below 3% for peak areas and below 1% for retention times. The experiments were performed in triplicate.

Antioxidant activity

DPPH radical scavenging assay

Antioxidant activity was determined using the DPPH radical scavenging assay. Extract solutions (5-1000 µg/mL) were mixed with 200 µM DPPH reagent in ratio (1:1, v/v) in a 96-well microplate and incubated in the dark at room temperature for 30 min. Absorbance was measured at 517 nm using a microplate reader. The half-maximal Inhibitory Concentration (IC_{50}) was calculated as the concentration required to scavenge 50% of DPPH radicals. Trolox was used as a positive control. The experiments were performed in triplicate in the same extract (Oktiansyah et al. 2023).

ABTS radical scavenging assay

The 7 mM ABTS radical cation ($ABTS^{\bullet+}$) was freshly prepared before analysis. Extracts (5-1000 µg/mL) were mixed with 7 mM $ABTS^{\bullet+}$ solution in ratio 1:1 into a 96-well microplate and incubated in the dark at room temperature for 10 min. Absorbance was recorded at 735 nm. IC_{50} values were calculated, and Trolox was used as a positive control. The experiments were performed in triplicate in the same extract (Saiprom et al. 2026).

Ferric-Reducing Antioxidant Power (FRAP)

The FRAP reagent was prepared by combining 300 mM acetate buffer (pH 3.6), 10 mM TPTZ dissolved in 40 mM HCl, and 20 mM $FeCl_3$ solution at a ratio of 10:1:1 (v/v/v). An extract at 100 µg/mL (20 µL) was added to the FRAP reagent (80 µL) in a 96-well microplate and incubated in the dark for 4 min. Absorbance was measured at 595 nm. Trolox was used as a positive control. The results were expressed as mmol Fe^{2+} per 100 g of extract (mmol Fe^{2+}/100 g extract). The test samples were calculated from the calibration plot of $FeSO^4$ (5-150 µM, y = 0.0233x - 0.0517; $R^2 = 0.9999$) (Rumpf et al. 2023). The experiments were performed in triplicate in the same extract

Antibacterial activity

Disc diffusion assay

Antibacterial activity was assessed using the disc diffusion method (Balouiri et al. 2016). Extracts were dissolved in 100% DMSO and serially two-fold diluted in Mueller-Hinton broth, with final DMSO concentration not exceeding 5% and 20 µL of extract solution (50 mg/mL) was applied per sterile 6-mm paper disc. Pure colonies of *E. coli* ATCC 25922 and *S. aureus* ATCC 25923 were adjusted to a 0.5 McFarland standard (approximately 1×10^8 CFU/mL) and spread onto Mueller-Hinton agar plates. The impregnated discs were placed on the inoculated agar surface and incubated at 37°C for 18-24 h. Gentamicin (10 µg/disc) was used as the positive control for *E. coli*, whereas penicillin (10 µg/disc) was used as the positive control for *S. aureus*. DMSO served as the negative control. All assays were performed in triplicate (n = 3) in the same extract. Antibacterial activity was expressed as inhibition zone diameter (mm) and reported as mean ± SD.

Table 2. Calibration equations, coefficients of determination (R^2), Limits of Detection (LOD), and Limits of Quantification (LOQ) of cannabinoid standards determined by HPLC

Standard cannabinoids	Linear equation	R^2 value	LOD (mg/L)	LOQ (mg/L)
CBDV	y = 13259.6x - 480.096	0.9996	0.14	0.43
CBDA	y = 24238.6x - 1288.65	0.9995	0.18	0.55
CBGA	y = 13098.9x - 768.586	0.9995	0.18	0.53
CBG	y = 12656.6x - 588.956	0.9996	0.20	0.59
CBD	y = 12835.8x - 565.245	0.9996	0.20	0.59
THCV	y = 12942.2x - 483.047	0.9996	0.20	0.62
CBN	y = 19782.9x - 1168.59	0.9994	0.12	0.37
Δ9-THC	y = 12708.8x - 255.379	0.9997	0.17	0.52
CBC	y = 11972.5x - 531.893	0.9995	0.20	0.60
THCA	y = 11069.7x - 532.213	0.9994	0.21	0.64

Note: The data from Chokchaisiri et al. (2026)

Determination of Minimum Inhibitory Concentration (MIC) and Minimum Bactericidal Concentration (MBC)

MIC and MBC were determined using the broth microdilution method (Balouiri et al. 2016). Based on the preliminary disc diffusion results, no inhibition zone was observed against *E. coli*, whereas measurable inhibition was detected for *S. aureus*. Therefore, MIC and MBC determinations were performed only for the susceptible strain (*S. aureus*) to further characterize its antibacterial response. Extracts were dissolved in DMSO and serially two-fold diluted in Mueller-Hinton broth, with final DMSO concentration not exceeding 5%. Fifty microliters of each dilution were dispensed into 96-well plates. *S. aureus* was adjusted to 0.5 McFarland (approximately 1×10^8 CFU/mL), diluted to 1×10^6 CFU/mL, and 50 µL were added to each well to obtain a final inoculum of 5×10^5 CFU/mL. Plates were incubated at 37°C for 18 h. MIC was defined as the lowest concentration showing no visible bacterial growth. For MBC determination, aliquots from wells without visible growth were subcultured on Mueller-Hinton agar and incubated at 37°C for 24 h. MBC was defined as the lowest concentration showing no bacterial growth. All experiments were performed in triplicate (n = 3).

Pharmacokinetic properties prediction

Pharmacokinetic properties of selected bioactive compounds identified in YKRB extracts were predicted using SwissADME (Molecular Modelling Group, Swiss Institute of Bioinformatics; https://www.swissadme.ch/). The analysis evaluated Absorption, Distribution, Metabolism, and Excretion (ADME) parameters, including drug-likeness, gastrointestinal absorption, and predicted bioavailability, to assess drug-likeness and pharmacokinetic behavior of major constituents (Jurowski et al. 2025).

Statistical analysis

Statistical analysis was performed using IBM SPSS Statistics version 23.0 (IBM Corp., Armonk, NY, USA). Data are presented as mean ± standard deviation (SD, n = 3). Data normality was assessed using the Shapiro-Wilk test, and homogeneity of variances was evaluated using Levene's test. When data met the assumptions of normality and homoscedasticity, differences among solvent extracts (hexane, ethyl acetate, and ethanol) for Total Phenolic Content (TPC), Total Flavonoid Content (TFC), Total Tannin Content (TTC), antioxidant activities (DPPH, ABTS, and FRAP), cannabinoid content, and inhibition zone diameters were evaluated using one-way Analysis of Variance (ANOVA) followed by Tukey's Honestly Significant Difference (HSD) test. A p-value < 0.05 was considered statistically significant. All experiments were conducted using the same extract preparation, and n = 3 represents three independent analytical measurements (technical replicates) performed for each extract in each assay.

Pearson correlation analysis between phytochemical contents (TPC, TTC, and TFC) and antioxidant activities (DPPH, ABTS, and FRAP assays) was performed. The correlation heatmap was generated based on Pearson's correlation coefficient with a significance level of $p < 0.05$ using the SRplot webserver (https://www.bioinformatics.com.cn/srplot, accessed on 8 May 2026) (Tang et al. 2023).

Principal Component Analysis (PCA) and Hierarchical Cluster Analysis (HCA) were performed using MetaboAnalyst 6.0 (https://www.metaboanalyst.ca/home.xhtml, accessed on 8 May 2026). All identified phytochemical compounds detected in YKRB extracts by GC-MS analysis were included in the PCA. Data were normalized by median normalization, log-transformed (base 10), and Pareto-scaled prior to analysis. Hierarchical clustering and dendrogram generation were subsequently performed using the hclust package.

RESULTS AND DISCUSSION

Extraction yield and solvent-dependent chemical diversity

Extraction yield of the YKRB remedy varied according to solvent polarity. The hexane extract produced the highest recovery (11.34%), followed by ethyl acetate (10.22%) and ethanol (7.75%). This pattern suggests that a considerable proportion of the extractable constituents in the formulation may possess low to intermediate polarity. Solvent polarity strongly influences extraction efficiency because non-polar solvents preferentially dissolve lipophilic metabolites, whereas polar solvents are generally more suitable for phenolic acids and related compounds (Khoddami et al. 2013).

Because *C. sativa* is one of the principal components of the formulation, the relatively higher yield obtained with hexane may partly be associated with the presence of lipophilic metabolites such as neutral cannabinoids (Pellati et al. 2018). However, as YKRB is a polyherbal preparation composed of multiple plant species, the observed extraction pattern likely reflects contributions from various phytochemical classes present in the formulation.

Overall, the results indicate that extraction solvent selection influences the range of chemical constituents recovered from a polyherbal remedy. Nevertheless, extraction yield reflects only the total mass of recovered constituents under specific solvent conditions and does not provide direct information about the chemical composition of the extracts. This solvent-dependent extraction pattern therefore highlights the chemical diversity that may be obtained from complex herbal formulations containing multiple botanical sources. Such variation in extracted phytochemical classes may contribute to the differences observed in antioxidant and antibacterial activities among the solvent fractions.

Total phenolic, flavonoid, and tannin contents

Total Phenolic Content (TPC) was highest in the ethanol extract (53.52 mg GAE/g extract), followed by ethyl acetate (51.80 mg GAE/g extract), whereas the hexane fraction showed the lowest value (41.59 mg GAE/g extract) (Table 3). This trend is generally consistent with

the preferential extraction of polar phenolic compounds in more polar solvents (Do et al. 2014).

Total Tannin Content (TTC) ranged from 62.71 to 71.61 mg TAE/g extract, with ethanol exhibiting the highest level. Although tannins are generally classified as polar polyphenols, their distribution across solvent fractions suggests structural diversity and variable solubility among tannin-type polyphenols. In Thai Traditional Medicine, herbs with an astringent taste are traditionally associated with diarrhea management. Previous studies have suggested that tannins can interact with mucosal proteins and may influence intestinal permeability (Cosme et al. 2025). The presence of measurable tannin levels in YKRB is therefore consistent with its traditional use; however, this study did not directly evaluate antidiarrheal mechanisms.

In contrast, TFC was highest in the hexane extract (61.09 mg QE/g extract). This observation suggests the possible presence of less polar or methoxylated flavonoid-type constituents in the non-polar fraction. Notably, the extract with the highest total phenolic content did not exhibit the strongest radical-scavenging activity, indicating that radical scavenging capacity may depend on the overall chemical composition rather than phenolic concentration alone. Similar observations have been reported in cannabis-derived extracts, where antioxidant activity is associated with multiple phytochemical classes (Mokoena et al. 2022). These findings further emphasize the chemical complexity of polyherbal formulations and the contribution of multiple metabolite classes to their biological properties. Notably, the higher TFC relative to TPC may reflect assay-specific responses and differences in calibration standards rather than true compositional abundance.

Phytochemical composition by GC-MS analysis

GC-MS analysis revealed that YKRB extracts contained multiple putatively identified phytochemical constituents, including cannabinoids detected across the solvent systems (Table 4). Tetrahydrocannabinol (THC) was detected as a relatively abundant constituent based on GC-MS peak area normalization (23.24-27.91%), followed by cannabinol (CBN) (14.18-21.06%), with smaller amounts of cannabidiol (CBD) and cannabichromene (CBC). However, the relative abundance of cannabinoids based on GC-MS peak area normalization should not be interpreted as indicative of dominant pharmacological contribution, as the extract represents a complex mixture of multiple phytochemical classes. Neutral lipophilic cannabinoids were enriched in the non-polar fraction, whereas semi-polar extracts contained relatively higher levels of lignan derivatives.

Macelignan was detected in all extracts, with the highest level observed in ethyl acetate (10.55%). This lignan, reported from *M. fragrans*, exhibits documented antioxidant and antimicrobial activities (Matulyte et al. 2020; Burgberger et al. 2025), suggesting that phenolic constituents derived from Myristicaceae may contribute to the observed phytochemical profile of the formulation.

Gingerenone A (2.41%) was detected in the ethanol extract. This phenolic compound reported from Zingiberaceae family has demonstrated antioxidant and anti-inflammatory properties and has been investigated as a potential inhibitor of *S. aureus* enzymatic targets (Rampogu et al. 2018). More recent studies report that gingerenone A can attenuate intestinal inflammation and support epithelial barrier integrity (Liang et al. 2024).

Cannabinoids have been reported to modulate oxidative pathways (Pereira et al. 2021) and influence enteric neuromuscular function through CB1/CB2 signaling, which regulates gastrointestinal motility and visceral sensitivity (Camilleri 2018). These reported biological properties may be relevant to the antioxidant activity observed in the present study and to the traditional use of this formulation for relieving intestinal colic and spasmodic bowel contraction. However, such effects were not investigated in the present study.

In addition to cannabinoids, the chromatographic profile also included lignans, terpenoid derivatives, and other lipophilic metabolites detected at varying peak areas across solvent fractions. The presence of compounds such as macelignan and ginger-derived phenolics highlights the contribution of non-cannabis botanical ingredients within the formulation. These observations indicate that YKRB extracts represent chemically complex mixtures rather than single-compound systems.

Overall, the co-occurrence of cannabinoids, lignans, and ginger-derived phenolics illustrates the chemical heterogeneity of this polyherbal remedy. Differences among solvent fractions further reflect the multi-component nature of the formulation derived from several botanical taxa. The coexistence of phytochemicals derived from multiple plant families emphasizes the inherent chemical diversity of traditional polyherbal formulations. Due to differences in ionization efficiency and detector response among compounds, direct quantitative comparison across different chemical classes should be interpreted with caution.

Table 3. Antioxidant activities and phytochemical contents of YKRB extracts

Parameter	Solvents			Trolox
	Hexane	EtOAc	EtOH	
DPPH; IC_{50} (µg/mL)	85.30 ± 0.53^{c}	56.72 ± 0.72^{b}	95.25 ± 2.23^{d}	7.35 ± 0.04^{a}
ABTS; IC_{50} (µg/mL)	23.26 ± 0.52^{b}	26.93 ± 0.72^{c}	26.03 ± 0.33^{c}	6.06 ± 0.05^{a}
FRAP (mmol Fe^{2+}/100 g extract)	119.30 ± 4.55^{c}	200.92 ± 12.84^{b}	131.82 ± 7.30^{c}	1642.08 ± 42.12^{a}
TPC (mg GAE/g extract)	41.59 ± 2.65^{b}	51.80 ± 3.37^{a}	53.52 ± 1.27^{a}	-
TTC (mg TAE/g extract)	68.40 ± 4.91^{a}	62.71 ± 5.11^{a}	71.61 ± 0.59^{a}	-
TFC (mg QE/g extract)	61.09 ± 0.31^{a}	59.28 ± 0.51^{b}	42.68 ± 0.51^{c}	-

Note: Values are expressed as mean ± SD (n = 3). Different superscript letters (a-d) within the same row indicate significant differences by Tukey's HSD test ($p < 0.05$)

Table 4. GC-MS-identified phytochemical constituents of YKRB extracts with hexane, ethyl acetate, and ethanol

Comp. No.	MW	Formula	KI	Compound name	% Peak area		
					Hexane	EtOAc	EtOH
1	152	$C_{10}H_{16}O$	1121	Camphor	-	0.19	-
2	220	$C_{15}H_{24}O$	1507	Caryophyllene oxide	-	0.37	0.24
3	206	$C_{14}H_{22}O$	1695	2,5,9-Trimethylcycloundeca-4,8-dienone	-	0.13	-
4	278	$C_{20}H_{38}$	1774	Neophytadiene	-	-	0.15
5	340	$C_{23}H_{32}O_2$	2788	Phenol,2,2'-methylenebis[6-(1,1-dimethylethyl)-4-methyl-	-	-	0.17
6	314	$C_{21}H_{30}O_2$	2605	Cannabidiol (CBD)	0.85	3.38	3.56
7	314	$C_{21}H_{30}O_2$	2486	Cannabichromene (CBC)	1.24	3.38	4.28
8	328	$C_{21}H_{28}O_3$	2490	Cannabicoumaronone	0.72	1.22	1.18
9	330	$C_{21}H_{30}O_3$	2587	Cannabielsoin A	-	0.34	-
10	314	$C_{21}H_{30}O_2$	2475	Tetrahydrocannabinol (THC)	23.24	25.42	27.91
11	310	$C_{21}H_{26}O_2$	2582	Cannabinol (CBN)	14.18	21.06	16.79
12	326	$C_{20}H_{22}O_4$	2524	5,5'-((2R,3S)-2,3-Dimethylbutane-1,4-diyl)bis(benzo[d][1,3]dioxole)	0.24	0.41	0.45
13	328	$C_{20}H_{24}O_4$	2589	Macelignan	6.34	10.55	8.00
14	330	$C_{20}H_{26}O_4$	2655	Meso-Dihydroguaiaretic Acid	1.70	2.58	-
15	356	$C_{21}H_{24}O_5$	3026	Gingerenone A	-	-	2.41
16	328	$C_{22}H_{32}O_2$	2603	3-Homotetrahydrocannibinol	0.26	-	-
17	388	$C_{22}H_{28}O_6$	2898	(1S,2R)-2-(4-Allyl-2,6-dimethoxyphenoxy)-1-(3,4-dimethoxyphenyl)propan-1-ol	-	0.44	0.35
18	520	$C_{28}H_{57}I$	3219	Octacosane,1-iodo-	-	0.27	-
19	758	$C_{54}H_{110}$	5389	Tetrapentacontane	-	-	0.28
20	380	$C_{24}H_{28}O_4$	2934	Cassumunene	0.23	0.39	0.72
21	412	$C_{29}H_{48}O$	2739	Stigmasterol	-	-	0.15
22	414	$C_{29}H_{50}O$	2731	γ-Sitosterol	0.49	0.88	0.79
23	426	$C_{30}H_{50}O$	2873	α-Amyrin		0.79	0.71
24	394	$C_{29}H_{46}$	2635	24-Noroleana-3,12-diene	0.84	-	1.39
25	424	$C_{30}H_{48}O$	2869	β-Amyrone	0.46	0.36	-
26	440	$C_{31}H_{52}O$	2834	9,19-Cyclolanostan-3-ol,24-methylene-,(3β)-	0.73	0.47	0.44
27	512	$C_{31}H_{60}O_5$	3600	Tetradecanoicacid,2-hydroxy-1,3-propanediylester	-	0.33	-
28	722	$C_{45}H_{86}O_6$	4932	Trimyristin	-	15.43	18.72

Table 5. Cannabinoid content of YKRB extracts analyzed by HPLC

Cannabinoids	Cannabinoid content (mg/g extract)		
	Hexane	EtOAc	EtOH
CBDV	ND	ND	ND
CBDA	ND	ND	ND
CBGA	ND	ND	ND
CBG	0.39±0.00^{a}	ND	ND
CBD	0.60±0.00^{c}	0.86±0.00^{b}	1.16±0.00^{a}
THCV	ND	ND	ND
CBN	4.82±0.01^{b}	4.55±0.00^{a}	4.90±0.01^{a}
Δ9-THC	6.92±0.01^{a}	2.01±0.01^{c}	4.10±0.00^{b}
CBC	1.21±0.02^{b}	1.02±0.00^{c}	1.37±0.01^{a}
THCA	2.00±0.04^{a}	ND	ND

Note: ND is not detected. Values are expressed as mean ± SD (n = 3). Different superscript letters (a-c) within the same row indicate significant differences by Tukey's HSD test ($p < 0.05$)

Cannabinoid contents by HPLC analysis

HPLC analysis confirmed solvent-dependent variation in cannabinoid composition (Table 5). Δ9-Tetrahydrocannabinol (Δ9-THC) was the most abundant quantified cannabinoid in all fractions, with the highest concentration detected in the hexane extract (6.92 mg/g extract), followed by the ethanol extract (4.10 mg/g extract) and the ethyl acetate extract (2.01 mg/g extract). This trend corresponds with the relatively high lipophilicity of neutral cannabinoids, which preferentially partition into non-polar solvents (Andre et al. 2016).

Cannabinol (CBN) was consistently detected across extracts (4.55-4.90 mg/g extract), suggesting a relatively stable distribution under the extraction conditions applied. Cannabidiol (CBD) and cannabichromene (CBC) were present at lower levels but showed relatively higher concentrations in ethanol extracts (CBD: 1.16 mg/g extract; CBC: 1.37 mg/g extract), which may reflect their slightly greater polarity relative to THC, associated with phenolic hydroxyl groups.

Cannabigerol (CBG, 0.39 mg/g extract) and tetrahydrocannabinolic acid (THCA, 2.00 mg/g extract) were detected exclusively in the hexane fraction, suggesting selective enrichment of neutral or weakly polar cannabinoids in non-polar solvents. Earlier studies describe antibacterial activity of CBG against Gram-positive bacteria (Farha et al. 2020) as well as antioxidant and anti-inflammatory properties of CBD and CBN (Appendino et al. 2008).

Overall, these results indicate that solvent polarity strongly influences cannabinoid partitioning within YKRB extracts. Although the hexane fraction contained the highest THC concentration, the largest inhibition zone against *S. aureus* was observed for the ethanol extract, suggesting that antibacterial activity is likely influenced by the combined composition of multiple phytochemical classes rather than cannabinoid content alone. Similarly, the relatively higher CBD and CBC levels in ethanol extracts may contribute to antioxidant activity; however, the present data do not establish direct causal relationships

between individual cannabinoids and the observed bioactivities. Differences among solvent fractions therefore reflect the variable contribution of cannabinoid subclasses within the broader phytochemical composition of the formulation.

Antioxidant capacity and phytochemical contribution

Antioxidant activity of YKRB extracts varied according to solvent polarity and the assay system used (Table 3). Based on the classification proposed by Sukweenadhi et al. (2020), antioxidant strength can be categorized as very strong (IC_{50} < 50 µg/mL), strong (50-100 µg/mL), moderate (101-150 µg/mL), and weak (>150 µg/mL).

In the DPPH assay (Table 3), the ethyl acetate extract (IC_{50} = 56.72 µg/mL), the hexane extract (85.30 µg/mL), and the ethanol extract (95.25 µg/mL) were all classified as strong antioxidants. In contrast, ABTS IC_{50} values ranged from 23.26 to 26.93 µg/mL, placing all extracts within the very strong antioxidant category according to the same classification scheme. Trolox exhibited substantially lower IC_{50} values, confirming the moderate potency of the crude extracts relative to the reference standard.

The difference between DPPH and ABTS responses may be attributable to assay-specific detection mechanisms. ABTS detects both hydrophilic and lipophilic antioxidants, whereas DPPH primarily measures hydrogen-donating activity in organic systems (Christodoulou et al. 2022). The relatively strong ABTS activity of the hexane fraction may indicate the presence of lipophilic antioxidant constituents. Cannabinoids such as CBD and THC have been reported to modulate oxidative pathways independently of classical phenolic hydroxyl density (Atalay et al. 2019; Pereira et al. 2021), which may contribute to the observed antioxidant responses; however, the overall activity is more likely attributable to the combined effects of multiple phytochemical classes present in the crude extract rather than individual cannabinoid constituents alone.

Although ethyl acetate and ethanol extracts contained higher total phenolic content (51.80-53.52 mg GAE/g extract), a simple direct relationship between phenolic concentration and radical scavenging activity was not apparent from the observed values across assays. FRAP results showed enhanced reducing capacity in the ethyl acetate fraction (200.92 mmol Fe^{2+}/100 g extract), which may reflect the presence of semi-polar phenolic constituents. Taken together, the antioxidant profile of YKRB likely reflects interactions among multiple phytochemical classes, including cannabinoids, phenolics, and flavonoids, rather than being determined by a single compound class. This observation is consistent with the concept that crude plant extracts exert biological activity through synergistic or additive interactions among diverse phytochemical constituents rather than single-compound effects.

Pearson's correlation analysis was performed to evaluate the relationship between the phytochemical contents of YKRB extracts and their antioxidant activities based on Pearson's correlation coefficient (r). A very strong positive correlation was observed between DPPH and FRAP assays with r = 0.95, indicating that the antioxidant compounds in the YKRB extracts may utilize similar mechanisms in scavenging radicals and reducing metal ions. The TPC exhibited a moderate positive correlation with the FRAP assay (r = 0.51), while a strong negative correlation (r = -0.94) was found between TPC and the ABTS assay (Figure 1). The negligible correlation between TPC and TTC (r = -0.03) indicated that tannins were not the predominant phenolic constituents. Furthermore, TTC showed strong negative correlations with the DPPH (r = -0.98) and FRAP (r = -0.87) assays. This finding may suggest that higher tannin concentrations could interfere with the radical-scavenging capacity of other phytochemicals present in the YKRB extracts.

Antibacterial activity

YKRB extracts exhibited detectable selective antibacterial activity against *S. aureus*, whereas no inhibition was observed against *E. coli* (Table 6, Figures 2 and 3). This pattern corresponds with structural differences between Gram-positive and Gram-negative bacteria. Gram-negative species possess an outer membrane enriched with lipopolysaccharides that functions as a permeability barrier, restricting the uptake of many hydrophobic compounds and antibacterial agents (Maher and Hassan 2023). In contrast, the absence of this outer membrane in Gram-positive bacteria allows greater accessibility of lipophilic molecules.

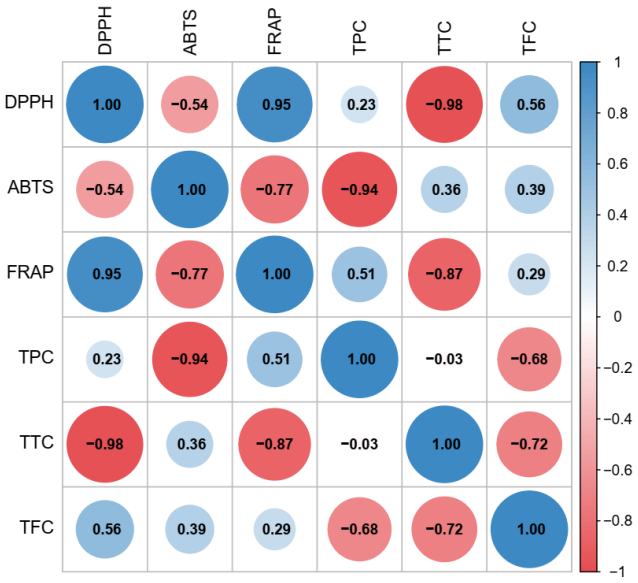

Figure 1. Pearson's correlation heatmap diagram between phytochemical contents (TPC, TTC, and TFC) and their antioxidant activities (DPPH, ABTS, and FRAP assay) of YKRB extract. The diagram was generated by SRplot webserver (https://www.bioinformatics.com.cn/srplot, accessed on 8 May 2026)

Table 6. Antibacterial activity of YKRB extracts against *Escherichia coli* and *Staphylococcus aureus* determined by the disc diffusion method (zone of inhibition, mm), Minimum Inhibitory Concentration (MIC) and Minimum Bactericidal Concentration (MBC)

Solvent	Zone of inhibition (mm)		MIC and MBC against *Staphylococcus aureus*	
	Escherichia coli	*Staphylococcus aureus*	MIC (mg/mL)	MBC (mg/mL)
Hexane	-	10.41 ± 0.30^{c}	25	50
EtOAc	-	9.39 ± 0.25^{d}	25	50
EtOH	-	12.42 ± 0.41^{b}	25	50
Gentamicin (10 µg/disc)	25.04 ± 0.02	-	-	-
Penicillin (10 µg/disc)	-	31.87 ± 0.02^{a}	-	-

Note: Values are expressed as mean ± SD (n = 3). Different superscript letters (a-d) within the same column indicate significant differences ($p < 0.05$). " - " indicates no inhibition zone observed. MIC and MBC were determined by the broth microdilution method (n = 3) and No activity was observed against *Escherichia coli*

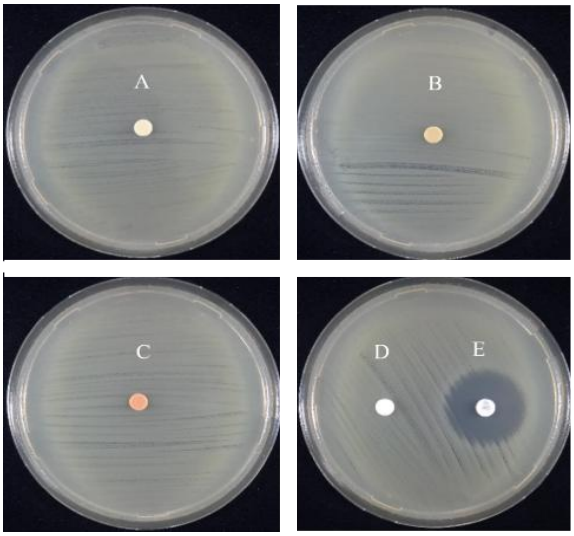

Figure 2. Disc diffusion assay against *Escherichia coli* demonstrating no inhibitory activity of YKRB extracts (50 mg/mL) from A. EtOH extract, B. EtOAc extract, and C. hexane extract, D. Penicillin (10 µg/disc) and E. Gentamicin (10 µg/disc) served as positive controls. This assay was performed in triplicate (n = 3).

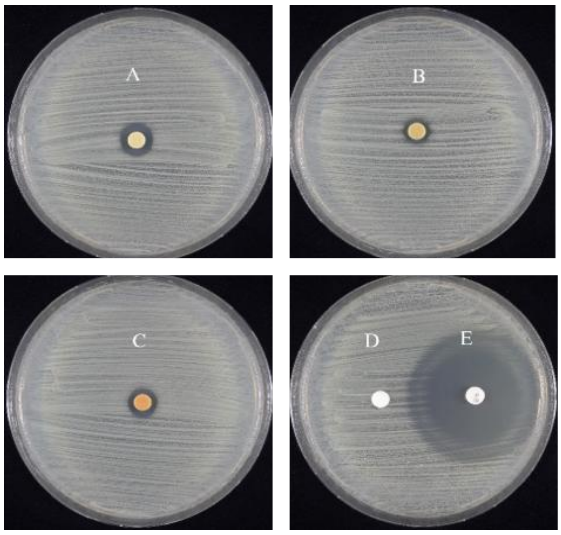

Figure 3. Disc diffusion assay against *Staphylococcus aureus* showing inhibition zones produced by YKRB extracts (50 mg/mL) from A. EtOH extract, B. EtOAc extract, and C. hexane extract. D. Gentamicin (10 µg/disc) and E. Penicillin (10 µg/disc) were used as positive controls. This assay was performed in triplicate (n = 3).

Phytochemical profiling indicated the presence of lipophilic cannabinoids and terpenoid constituents, particularly in non-polar fractions. Cannabinoids such as cannabidiol and cannabigerol have been reported to display preferential activity against Gram-positive bacteria, partly through membrane-associated interactions (Farha et al. 2020; Blaskovich et al. 2021). However, the present study did not perform activity-guided fractionation or compound isolation, and therefore no direct causal relationship between individual constituents and the observed antibacterial activity can be established. The inhibition zones observed against *S. aureus* (9.39-12.42 mm) correspond to moderate antibacterial activity typical of crude plant extracts and should not be interpreted as high potency.

Broth microdilution assays produced MIC and MBC values of 25 mg/mL and 50 mg/mL, respectively (Table 6). Similar MIC and MBC values across solvent extracts may suggest comparable bacteriostatic and bactericidal thresholds within the tested concentration range. Compared with purified cannabinoids that exhibit MIC values in the low µg/mL range (Appendino et al. 2008; Farha et al. 2020), the higher concentrations observed here are expected for crude polyherbal extracts, in which active constituents represent only a portion of the total extract mass. Therefore, the observed activity should be interpreted as indicative of preliminary screening rather than therapeutic-level antibacterial effectiveness.

Although the activity was lower than that of penicillin, a β-lactam antibiotic targeting penicillin-binding proteins (Bush and Bradford 2016), the results suggest that antibacterial effects may at least partially involve membrane-associated interactions rather than classical enzyme-targeting mechanisms. However, this mechanistic interpretation remains speculative and was not directly investigated in the present study. Redox-active phytochemicals can also influence bacterial membrane stability and oxidative balance (Burt 2004), which may contribute to the observed selective inhibition.

These findings are limited to the tested reference strains and should not be generalized to broader bacterial populations. In addition, only one Gram-positive and one Gram-negative strain were evaluated in this study, and therefore the antibacterial findings should be considered preliminary within this limited experimental scope.

Overall, the antibacterial activity of YKRB should be interpreted as moderate and preliminary, and the observed

inhibition against *S. aureus* reflects selective activity against a Gram-positive model strain rather than broad-spectrum antibacterial efficacy. In addition, the use of technical replicates based on a single extract batch limits the generalizability of the findings. Further fractionation and mechanistic studies are required to identify the principal active constituents. Importantly, this study did not directly evaluate antidiarrheal activity, and therefore no therapeutic conclusions related to gastrointestinal efficacy can be drawn.

Physicochemical properties and ADME prediction

The physicochemical properties and Lipinski's rule of chemical constituent showed in Table 7. The physicochemical and drug-likeness analysis revealed that most identified compounds complied with Lipinski's Rule of Five, indicating favorable oral drug-like properties. Several compounds, including Cannabidiol (CBD), Cannabielsoin A, Macelignan, and Gingerenone A, showed no Lipinski violations and demonstrated suitable molecular weight, polarity, and hydrogen bonding characteristics. In contrast, highly lipophilic compounds such as Stigmasterol, α-Amyrin, and Trimyristin exhibited poor aqueous solubility and multiple Lipinski violations, suggesting limited oral bioavailability. Overall, cannabinoid and phenolic compounds displayed promising potential for further pharmacological development.

In silico ADME analysis indicated that several phytochemicals identified in YKRB showed predicted gastrointestinal (GI) absorption, including cannabinoids and phenolic constituents (Table 8). However, these predictions represent computational estimates and should be interpreted as preliminary screening results rather than evidence of actual absorption. This observation is broadly consistent with the traditional oral administration of the YKRB remedy, suggesting that some constituents may be potentially available for absorption following oral intake. In contrast, larger sterols and triterpenoids such as α-amyrin, β-amyrone, and γ-sitosterol showed low predicted GI absorption, indicating limited predicted systemic availability under these in silico conditions.

Several cannabinoids and phenolic constituents were also predicted to inhibit multiple cytochrome P450 (CYP) isoforms, particularly CYP2C9, CYP2C19, and CYP2D6 (Table 8). These predictions are consistent with previous reports that cannabinoids may interact with CYP-mediated drug metabolism (Stout and Cimino 2014; Zendulka et al. 2016). Such interactions suggest a potential for herb-drug interactions; however, this remains speculative and requires experimental validation, particularly when cannabinoid-containing herbal remedies are co-administered with conventional medications metabolized by CYP enzymes.

Table 7. Predicted physicochemical properties and Lipinski rule-of-five evaluation of selected phytoconstituents in YKRB

Compound name	MW	TPSA	HBA	HBD	LogP	LogS	Lipinski violations
Camphor	152	17.07	1	0	2.37	-2.16	0
Caryophyllene oxide	220	12.53	1	0	3.68	-3.45	0
2,5,9-Trimethylcycloundeca-4,8-dienone	206	17.07	1	0	3.26	-2.91	0
Neophytadiene	278	0	0	0	7.07	-6.77	1
Phenol,2,2'-methylenebis[6-(1,1-dimethylethyl)-4-methyl-	340	40.46	2	2	5.59	-5.98	1
Cannabidiol (CBD)	314	40.46	2	2	5.20	-5.69	1
Cannabichromene (CBC)	314	29.46	2	1	5.45	-5.84	1
Cannabicoumaronone	328	39.44	3	0	4.91	-4.95	0
Cannabielsoin A	330	49.69	3	2	4.36	-5.16	0
Tetrahydrocannabinol (THC)	314	29.46	2	1	5.33	-6.11	1
Cannabinol (CBN)	310	29.46	2	1	5.21	-5.74	1
5,5'-((2R,3S)-2,3-Dimethylbutane-1,4-diyl)bis(benzo[d][1,3]dioxole)	326	36.92	4	0	4.45	-5.27	0
Macelignan	328	47.92	4	1	4.25	-5.10	0
Meso-Dihydroguaiaretic Acid	330	58.92	4	2	4.09	-4.92	0
Gingerenone A	356	75.99	5	2	3.65	-4.15	0
3-Homotetrahydrocannibinol	328	29.46	2	1	5.56	-5.63	1
(1S,2R)-2-(4-Allyl-2,6-dimethoxyphenoxy)-1-(3,4-dimethoxyphenyl)propan-1-ol	388	66.38	6	1	3.69	-4.51	0
Octacosane,1-iodo-	520	0	0	0	11.26	-11.48	2
Tetrapentacontane	758	0	0	0	20.05	-19.36	2
Cassumunene	380	36.92	4	0	4.82	-5.61	0
Stigmasterol	412	20.23	1	1	6.98	-7.46	1
γ-Sitosterol	414	20.23	1	1	7.24	-7.90	1
α-Amyrin	426	20.23	1	1	7.05	-8.16	1
24-Noroleana-3,12-diene	394	0	0	0	7.55	-8.11	1
β-Amyrone	424	17.07	1	0	7.21	-8.04	1
9,19-Cyclolanostan-3-ol,24-methylene-,(3.β.)-	440	20.23	1	1	7.80	-8.74	1
Tetradecanoicacid,2-hydroxy-1,3-propanediylester	512	72.83	5	1	8.63	-8.52	2
Trimyristin	722	78.9	6	0	13.26	-13.19	2

Note: Lipinski criteria: MW ≤ 500; TPSA ≤ 140 Å; HBA ≤ 10; HBD ≤ 5; LogP ≤ 5; acceptable violations ≤ 1

Table 8. Predicted ADME properties and CYP450 inhibition profiles of selected phytoconstituents in YKRB

Compound name	GI absorption	BBB permeant	CYP1A2 inhibitor	CYP2C19 inhibitor	CYP2C9 inhibitor	CYP2D6 inhibitor	CYP3A4 inhibitor
Camphor	High	Yes	No	No	No	No	No
Caryophyllene oxide	High	Yes	No	Yes	Yes	No	No
2,5,9-Trimethylcycloundeca-4,8-dienone	High	Yes	No	No	No	No	No
Neophytadiene	Low	No	No	No	Yes	No	No
Phenol,2,2'-methylenebis[6-(1,1-dimethylethyl)-4-methyl-	High	Yes	No	Yes	No	Yes	No
Cannabidiol (CBD)	High	Yes	No	Yes	Yes	Yes	Yes
Cannabichromene (CBC)	High	No	No	No	Yes	Yes	Yes
Cannabicoumaronone	High	Yes	No	No	Yes	Yes	Yes
Cannabielsoin A	High	Yes	No	No	Yes	Yes	No
Tetrahydrocannabinol (THC)	High	Yes	No	Yes	Yes	Yes	No
Cannabinol (CBN)	High	Yes	Yes	Yes	No	Yes	No
5,5'-((2R,3S)-2,3-Dimethylbutane-1,4-diyl)bis(benzo[d][1,3]dioxole)	High	Yes	No	Yes	Yes	Yes	Yes
Macelignan	High	Yes	No	Yes	Yes	Yes	No
Meso-Dihydroguaiaretic Acid	High	Yes	Yes	Yes	No	Yes	Yes
Gingerenone A	High	Yes	Yes	No	Yes	Yes	Yes
3-Homotetrahydrocannibinol	High	No	No	No	No	Yes	No
(1S,2R)-2-(4-Allyl-2,6-dimethoxyphenoxy)-1-(3,4-dimethoxyphenyl)propan-1-ol	High	Yes	No	No	No	Yes	Yes
Octacosane,1-iodo-	Low	No	No	No	No	No	No
Tetrapentacontane	Low	No	No	No	No	No	No
Cassumunene	High	Yes	No	No	Yes	Yes	Yes
Stigmasterol	Low	No	No	No	Yes	No	No
γ-Sitosterol	Low	No	No	No	No	No	No
α-Amyrin	Low	No	No	No	No	No	No
24-Noroleana-3,12-diene	Low	No	No	No	No	No	No
β-Amyrone	Low	No	No	No	No	No	No
9,19-Cyclolanostan-3-ol,24-methylene-,(3.β.)-	Low	No	No	No	No	No	No
Tetradecanoicacid,2-hydroxy-1,3-propanediylester	Low	No	No	No	No	No	No
Trimyristin	Low	No	No	No	No	No	No

BOILED-Egg modeling predicted potential blood-brain barrier permeability for some neutral cannabinoids (Figure 4). Nevertheless, given that YKRB is traditionally used for gastrointestinal conditions, the relevance of BBB permeability is considered secondary and not central to the present study. Overall, the ADME results provide supportive computational insight into the physicochemical and pharmacokinetic tendencies of selected constituents but should not be interpreted as functional pharmacokinetic evidence. These predictions require further experimental validation and should be interpreted with caution.

The ADME analysis is therefore presented as a complementary computational assessment rather than a primary determinant of biological activity in this study.

Multivariate and clustering analysis

Principal component analysis (PCA) was performed to investigate patterns of similarity and variation among the identified phytochemical constituents of YKRB extracts obtained using hexane, ethyl acetate (EtOAc), and ethanol (EtOH) based on GC-MS analysis. The PCA biplot consisted of two principal components (PCs), with PC1 and PC2 accounting for 56.3% and 43.7% of the total variance, respectively (Figure 5). PC1 was mainly associated with compounds predominantly detected in the ethanol extract, whereas compounds identified in the ethyl acetate extract contributed mainly to PC2. Gingerenone A (compound 15) showed a strong correlation with compounds 5, 19, 4, and 21, which were detected exclusively in the ethanol extract and contributed positively to PC1. Cannabielsoin A (compound 9) showed a strong correlation with compounds 27, 18, 1, and 3, which were detected only in the ethyl acetate extract and contributed to the separation of this fraction from compounds 28, 23, 17, and 2, which were detected in both ethanol and ethyl acetate extracts. Compound 16, detected exclusively in the hexane extract, showed a strong correlation with cannabinoids and macelignan. Macelignan (compound 13) exhibited correlations with cannabinoids, including CBD (6), THC (10), and CBN (11), as well as compounds 26, 9, 12, 22, and 8, which were separated from other phytochemical groups (Figure 6). Based on the major contributions of phytochemical constituents to each principal component, the PCA score plot revealed three distinct clusters corresponding to the ethanol (cluster I), ethyl acetate (cluster II), and hexane (cluster III) extracts. Furthermore, hierarchical cluster analysis (HCA) was performed to confirm the clustering patterns observed in the PCA plot.

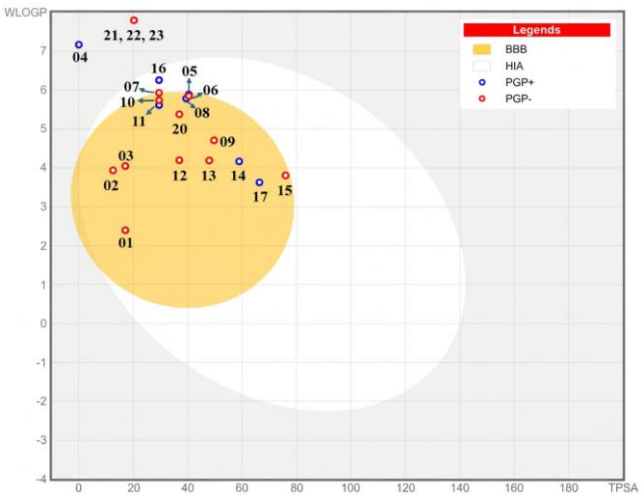

Figure 4. BOILED-Egg plot showing predicted gastrointestinal absorption (white region) and blood-brain barrier permeability (yellow region) of selected YKRB phytoconstituents. BBB is blood-brain barrier permeant, HIA is human intestinal absorption, PGP+ (blue dots) indicates compounds predicted to be effluxed from the CNS by P-glycoprotein, whereas PGP− (red dots) indicates compounds not predicted to undergo P-glycoprotein-mediated efflux

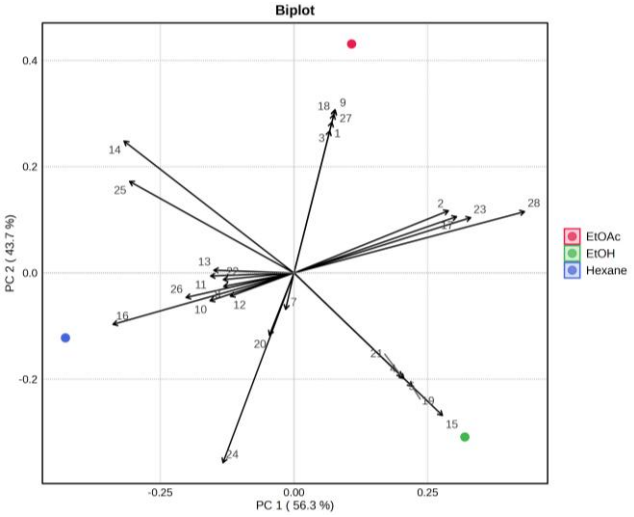

Figure 5. PCA biplot of the identified phytochemical constituents of YKRB extracts form hexane, ethyl acetate (EtOAc), and ethanol (EtOH) via GC-MS analysis

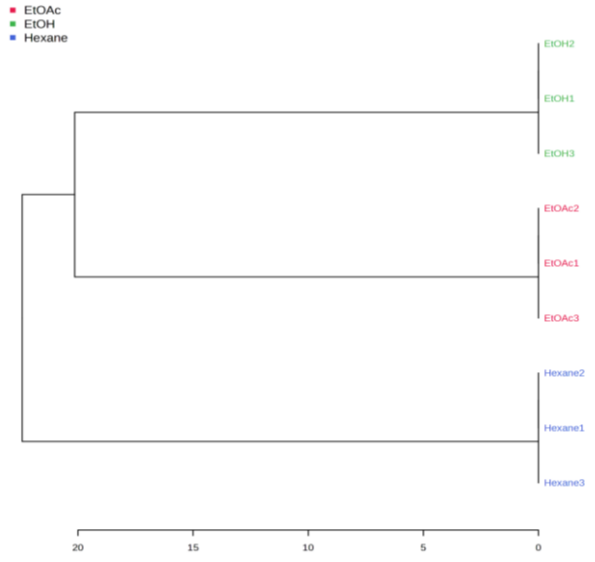

Figure 6. Hierarchical cluster analysis (HCA) of the identified phytochemical constituents of YKRB extracts form hexane, ethyl acetate (EtOAc), and ethanol (EtOH) via GC-MS analysis

Several limitations of the present study should be acknowledged. While this study provides initial insight into the phytochemical composition and biological properties of YKRB, the phytochemical profile was primarily based on GC-MS and HPLC analyses and may not fully represent non-volatile or thermolabile constituents. Antioxidant and antibacterial activities were evaluated using in vitro assays with a limited number of bacterial strains, specifically one Gram-positive and one Gram-negative reference strain. They therefore may not fully reflect in vivo biological responses. The ADME assessment relied on computational prediction without experimental pharmacokinetic validation. In addition, isolation of individual compounds and evaluation of synergistic interactions were not performed, which may influence the overall bioactivity profile. This study did not directly evaluate antidiarrheal activity, intestinal inflammation, epithelial barrier function, or disease-specific gastrointestinal models. Accordingly, the findings should be interpreted as preliminary evidence of chemical and biological properties rather than direct therapeutic efficacy. Further studies involving bioactive fractionation, in vivo models, and pharmacokinetic validation are warranted to confirm and extend these observations.

In conclusion, the results demonstrated that EtOH extracted the highest chemical components, which showed clear solvent-dependent differences in extraction yield and phytochemical composition, with cannabinoids and other lipophilic constituents enriched in non-polar fractions. Antioxidant assays (DPPH, ABTS, and FRAP) indicated measurable in vitro antioxidant activity, with variation depending on solvent polarity and assay system. Moreover, YKRB showed selective antibacterial activity against *S. aureus*, while no inhibition was observed against *E. coli*. The findings primarily highlight solvent-dependent phytochemical diversity and provide preliminary evidence of antioxidant and selective antibacterial properties of YKRB extracts. In silico ADME analysis was included as a supportive computational assessment and should not be interpreted as direct pharmacokinetic evidence. Overall, the results provide a preliminary chemical and biological basis for this traditional formulation and support future mechanistic and pharmacological investigations. However, because this study was limited to in vitro and computational analyses, further bioactivity, pharmacokinetic, and in vivo studies are required to confirm the findings.

ACKNOWLEDGEMENTS

The authors gratefully acknowledge Taratera Corporation Co., Ltd. for providing the *C. sativa* inflorescence used in this study. We sincerely thank the Department of Thai Traditional and Alternative Medicine, Ministry of Public Health, Thailand, for their support in compiling and translating classical Thai medicinal manuscripts. The authors also express their appreciation to Dr. Rumrada Meeboonya for assistance in plant identification and taxonomic verification.

REFERENCES

Alves FS, Cruz JN, de Farias Ramos IN, do Nascimento Brandão DL, Queiroz RN, da Silva GV, da Silva GV, Dolabela MF, da Costa ML, Khayat AS, de Arimatéia Rodrigues do Rego J. 2023. Evaluation of antimicrobial activity and cytotoxicity effects of extracts of *Piper nigrum* L. and piperine. Separations 10 (1): 21. https://doi.org/10.3390/separations10010021.

Andre CM, Hausman JF, Guerriero G. 2016. *Cannabis sativa*: The plant of the thousand and one molecules. Front Plant Sci 7: 19. https://doi.org/10.3389/fpls.2016.00019.

Appendino G, Gibbons S, Giana A, Pagani A, Grassi G, Stavri M, Smith E, Rahman MM. 2008. Antibacterial cannabinoids from *Cannabis sativa*: A structure-activity study. J Nat Prod 71 (8): 1427-1430. https://doi.org/10.1021/np8002673.

Asyhar R, Minarni M, Arista RA, Nurcholis W. 2023. Total phenolic and flavonoid contents and their antioxidant capacity of *Curcuma xanthorrhiza* accessions from Jambi. Biodiversitas 24 (9): 5007-5014. https://doi.org/10.13057/biodiv/d240944.

Atalay S, Jarocka-Karpowicz I, Skrzydlewska E. 2019. Antioxidative and anti-inflammatory properties of cannabidiol. Antioxidants 9 (1): 21. https://doi.org/10.3390/antiox9010021.

Balouiri M, Sadiki M, Ibnsouda SK. 2016. Methods for in vitro evaluating antimicrobial activity: A review. J Pharm Anal 6 (2): 71-79. https://doi.org/10.1016/j.jpha.2015.11.005.

Bhatwalkar SB, Mondal R, Krishna SBN, Adam JK, Govender P, Anupam R. 2021. Antibacterial properties of organosulfur compounds of garlic (*Allium sativum*). Front Microbiol 12: 613077. https://doi.org/10.3389/fmicb.2021.613077.

Blaskovich MAT, Kavanagh AM, Elliott AG, Zhang B, Ramu S, Amado M, Lowe GJ, Hinton AO, Pham DMT, Zuegg J, Beare N, Quach D, Sharp MD, Pugliano J, Rogers AP, Lyras D, Tan L, West NP, Crawford DW, Peterson ML, Callahan M, Thurn M. 2021. The antimicrobial potential of cannabidiol. Commun Biol 4: 7. https://doi.org/10.1038/s42003-020-01530-y.

Burgberger M, Mierziak J, Augustyniak B, Wojtasik W, Kulma A. 2025. The power of lignans: Plant compounds with multifaceted health-promoting effects. Metabolites 15 (9): 589. https://doi.org/10.3390/metabo15090589.

Burt S. 2004. Essential oils: Their antibacterial properties and potential applications in foods. Int J Food Microbiol 94 (3): 223-253. https://doi.org/10.1016/j.ijfoodmicro.2004.03.022.

Bush K, Bradford PA. 2016. β-Lactams and β-lactamase inhibitors: An overview. Cold Spring Harb Perspect Med 6 (8): a025247. https://doi.org/10.1101/cshperspect.a025247

Camilleri M. 2018. Cannabinoids and gastrointestinal motility: Pharmacology, clinical effects, and potential therapeutics in humans. Neurogastroenterol Motil 30 (9): e13370. https://doi.org/10.1111/nmo.13370.

Chokchaisiri S, Ngivprom U, Phatthanaphong P, Boon-orn K, Wongsonthom S, Chimpalee P. 2026. Phytochemical profiles and antioxidant activities of four *Cannabis sativa* cultivars in Thailand. Biodiversitas 27 (1): 1-8. https://doi.org/10.13057/biodiv/d270100.

Christodoulou MC, Orellana Palacios JC, Hesami G, Jafarzadeh S, Lorenzo JM, Domínguez R, Moreno A, Hadidi M. 2022. Spectrophotometric methods for measurement of antioxidant activity in food and pharmaceuticals. Antioxidants (Basel) 11 (11): 2213. https://doi.org/10.3390/antiox11112213.

Cosme F, Aires A, Pinto T, Oliveira I, Vilela A, Gonçalves B. 2025. A comprehensive review of bioactive tannins in foods and beverages. Molecules 30 (4): 800. https://doi.org/10.3390/molecules30040800.

Crowley K, Kiraga Ł, Miszczuk E, Skiba S, Banach J, Latek U, Mendel M, Chłopecka M. 2024. Effects of cannabinoids on intestinal motility, barrier permeability and therapeutic potential in gastrointestinal diseases. Intl J Mol Sci 25 (12): 6682. https://doi.org/10.3390/ijms25126682.

Department of Thai Traditional and Alternative Medicine. 2021. Collection of Conserved Thai Traditional Medicine Wisdom: National Thai Medicine Formulas Incorporating Cannabis. Ministry of Public Health, Nonthaburi.

Do QD, Angkawijaya AE, Tran-Nguyen PL, Huynh LH, Soetaredjo FE, Ismadji S, Ju YH. 2014. Effect of extraction solvent on total phenol content and antioxidant activity. J Food Drug Anal 22 (3): 296-302. https://doi.org/10.1016/j.jfda.2013.11.001.

Farha MA, El-Halfawy OM, Gale RT, MacNair CR, Carfrae LA, Zhang X, Jentsch NG, Magolan J, Brown ED. 2020. Uncovering the hidden antibiotic potential of *Cannabis*. ACS Infect Dis 6 (3): 338-346. https://doi.org/10.1021/acsinfecdis.9b00419.

Gomes CL, Silva CCAR, Melo CG, Ferreira MRA, Soares LAL, DA Silva RMF, Rolim LA, Rolim Neto PJ. 2021. Development of an analytical method for determination of polyphenols and total tannins from leaves of *Syzygium cumini* L. Skeels. An Acad Bras Cienc 93 (2): e20190373. https://doi.org/10.1590/0001-3765202120190373.

Jin S, Xu H, Yang C, O K. 2024. Regulation of oxidative stress in the intestine of piglets after enterotoxigenic *Escherichia coli* (ETEC) infection. Biochim Biophys Acta Mol Cell Res 1871 (5): 119711. https://doi.org/10.1016/j.bbamcr.2024.119711.

Jurowski K, Kobylarz D, Noga M. 2025. ADME profile of BZP (benzylpiperazine) - first application of multi-in silico approach methodology for comprehensive prediction of ADME profile (absorption, distribution, metabolism and excretion) important for clinical toxicology and forensic purposes. Chem Biol Interact 421: 111775. https://doi.org/10.1016/j.cbi.2025.111775.

Khoddami A, Wilkes MA, Roberts TH. 2013. Techniques for analysis of plant phenolic compounds. Molecules 18 (2): 2328-2375. https://doi.org/10.3390/molecules18022328.

Liang J, Dai W, Liu C, Wen Y, Chen C, Xu Y, Huang S, Hou S, Li C, Chen Y, Wang W, Tang H. 2024. Gingerenone A attenuates ulcerative colitis via targeting IL-17RA to inhibit inflammation and restore intestinal barrier function. Adv Sci (Weinh) 11 (28): e2400206. https://doi.org/10.1002/advs.202400206.

Maher C, Hassan KA. 2023. The gram-negative permeability barrier: Tipping the balance of the in and the out. mBio 14 (6): e0120523. https://doi.org/10.1128/mbio.01205-23.

Matulyte I, Jekabsone A, Jankauskaite L, Zavistanaviciute P, Sakiene V, Bartkiene E, Ruzauskas M, Kopustinskiene DM, Santini A, Bernatoniene J. 2020. The essential oil and hydrolats from *Myristica fragrans* seeds with magnesium aluminometasilicate as excipient: Antioxidant, antibacterial, and anti-inflammatory activity. Foods 9 (1): 37. https://doi.org/10.3390/foods9010037.

Ministry of Public Health. 2016. The Announcement to Define the Thailand National Traditional Medicine Textbook and Thailand National Traditional Pharmacopoeia. Department for Development of Thai Traditional and Alternative Medicine, Ministry of Public Health, Bangkok.

Mokoena D, George BP, Abrahamse H. 2022. The role of *Cannabis* species on oxidative stress in cancer cells. In: Chakraborti S (eds). Handbook of Oxidative Stress in Cancer. Springer, Singapore. https://doi.org/10.1007/978-981-16-5422-0_201.

Oktiansyah R, Elfita, Widjajanti H, Salni, Setiawan A. 2023. Antibacterial and antioxidant activity of endophytic fungi isolated the petiole of sungkai plant (*Peronema canescens*). Biodiversitas 24 (12): 6516-6526. https://doi.org/10.13057/biodiv/d241213.

Pellati F, Brighenti V, Sperlea J, Marchetti L, Bertelli D, Benvenuti S. 2018. New methods for comprehensive analysis of bioactive compounds in *Cannabis sativa*. Molecules 23 (10): 2639. https://doi.org/10.3390/molecules23102639.

Pereira SR, Hackett B, O'Driscoll DN, Sun MC, Downer EJ. 2021. Cannabidiol modulation of oxidative stress and signalling. Neuronal Signal 5 (3): NS20200080. https://doi.org/10.1042/NS20200080.

POWO. 2024. "Plants of the World Online. Facilitated by the Royal Botanic Gardens, Kew. https://powo.science.kew.org/

Rampogu S, Baek A, Gajula RG, Zeb A, Bavi RS, Kumar R, Kim Y, Kwon YJ, Lee KW. 2018. Ginger (*Zingiber officinale*) phytochemicals

gingerenone-A and shogaol inhibit SaHPPK: Molecular docking, molecular dynamics simulations and in vitro approaches. Ann Clin Microbiol Antimicrob 17 (1): 16. https://doi.org/10.1186/s12941-018-0266-9.

Rezvani M. 2024. Oxidative stress-induced gastrointestinal diseases: Biology and nanomedicines-a review. BioChem 4 (3): 189-216. https://doi.org/10.3390/biochem4030010.

Royal Thai Government Gazette. 2019. Narcotics Act No. 7 B.E. 2562 (2019). Government of Thailand, Bangkok.

Rumpf J, Burger R, Schulze M. 2023. Statistical evaluation of DPPH, ABTS, FRAP, and Folin-Ciocalteu assays to assess the antioxidant capacity of lignins. Intl J Biol Macromol 233: 123470. https://doi.org/10.1016/j.ijbiomac.2023.123470.

Saiprom Y, Fakkham S, Promsorn T, Krutchangthong S, Yongram C, Puthongking P. 2026. The effect of solvent extraction on chemical composition, antioxidant, alpha-glucosidase and nitric oxide inhibitor activities of Jindamanee, a Thai traditional formulation. Trop J Nat Prod Res 10 (1): 6778-6784. https://doi:10.26538/tjnpr/v10i1.48.

Stout SM, Cimino NM. 2014. Exogenous cannabinoids as substrates, inhibitors, and inducers of human drug metabolizing enzymes: A systematic review. Drug Metab Rev 46 (1): 86-95. https://doi.org/10.3109/03602532.2013.849268.

Sukweenadhi J, Yunita O, Setiawan F, Kartini, Siagian MT, Danduru AP, Avanti C. 2020. Antioxidant activity screening of seven Indonesian herbal extract. Biodiversitas 21 (5): 2062-2067. https://doi.org/10.13057/biodiv/d210532.

Tang D, Chen M, Huang X, Zhang G, Zeng L, Zhang G, Wu S, Wang Y. 2023. SRplot: A free online platform for data visualization and graphing. PLoS One 18 (11): e0294236. https://doi.org/10.1371/journal.pone.0294236.

Thai Traditional Medicine Institute. 2025. Reference Textbook of Thai Traditional Medicine. Ministry of Public Health, Nonthaburi, Thailand.

World Health Organization (WHO). 2023. Diarrhoeal Disease. WHO, Geneva. https://www.who.int.

Yongram C, Sripan P, Chokchaisiri S, Wonganan O, Meeboonya R, Kamoltham T, Krutchangthong S, Panyatip P. 2025. Antioxidant activity and phytochemical composition of Thai traditional *Cannabis* longevity recipes: In vitro evaluation of the Phontecho remedy. Trop J Nat Prod Res 9 (12): 6166-6174. https://doi.org/10.26538/tjnpr/v9i12.33.

Zendulka O, Dovrtělová G, Nosková K, Turjap M, Šulcová A, Hanuš L, Juřica J. 2016. Cannabinoids and cytochrome P450 interactions. Curr Drug Metab 17 (3): 206-226. https://doi.org/10.2174/1389200217666151210142051.